

Supporting Information

Carbon Dot-Sensitized Photoanodes for Visible Light-Driven Organic Transformations

Francisco Yarur Villanueva, John Manioudakis, Rafik Naccache, Marek B. Majewski*

Department of Chemistry and Biochemistry and Centre for NanoScience Research, Concordia University, Montreal, QC, Canada, H4B 1R6

* = Corresponding author (email: marek.majewski@concordia.ca)

Synthesis of Zinc Oxide Nanoparticles:

ZnO NPs were synthesized from zinc chloride, linoleic acid and sodium hydroxide in ethanol following a previously reported procedure.¹ ZnCl₂ (0.50 g, 3.7 mmol) was dissolved in deionized H₂O (7 mL) through sonication for 5 min. Then, NaOH (0.50 g, 12.5 mmol) and linoleic acid (4 mL, 12.8 mmol) were combined in ethanol (16 mL) and sonicated until the solution was clear. Both solutions were then mixed and held under constant stirring for 30 min. The final product was separated by centrifugation at 7000 rpm and then dispersed (2×) in ethanol to remove any unreacted material, followed by centrifugation. The final product was air dried overnight to yield a white powder.

Optimization of ZnO NW Growth:

The growing time of the ZnO NWs was optimized to minimize the electron-hole recombination and to facilitate the carrier collection pathways. It was observed that NWs achieve their optimal length after 3 hrs of growth (1.3 μm) where the NWs are tightly packed and highly oriented, while less than 3 hrs of growth results in arrays of disordered wires (Figure S19). More than 3 hrs of growth results in taller wires that may diminish the semiconducting properties of the device. In addition, the number of drops of ZnO NPs dispersion used for spin-coating the FTO films was also optimized. It was determined that three cycles of two drops per spin-coating cycle was the optimal number of drops in order to obtain uniform films of wires while keeping the aggregation of particles at minimum (Figures S19 and S20).

Synthesis of other CDs for the comparative study:

The green CDs were synthesized from a previously reported procedure.² Briefly, 20 mL of a 0.1 M solution of glutathione in formamide was prepared and sonicated until the solution became clear. A 10 mL sample was then placed in a microwave reaction vessel (35 mL capacity). The solution was heated in a microwave reactor at 180 °C for 5 min. The dark green product was then subjected to dialysis for 5 days in Millipore water to remove impurities. After dialysis, the product was concentrated in vacuo at 50 °C until the volume was reduced to 3 mL. Then three organic washes with acetone (99%) were performed to further purify the CDs. The product was left to air dry and then was resuspended in water or ethanol for further experiments.

The red CDs are synthesized from citric acid and formamide. Briefly, citric acid (5 g, 26 mmol) was dissolved in methanol (75 mL) and formamide (25 mL) was added. The solution was homogenized by stirring for 5 min, then, the solution was transferred to a hydrothermal reactor and the reaction was carried out at 180 °C for 4 hrs with stirring at 300 rpm. The product is a black liquid which was dialyzed for 5 days in Millipore water. Then, the solution was concentrated to 5 mL and three organic washes with acetone (99%) were performed to remove impurities. The product was then left in an oven to dry at 70 °C and resuspended in water or ethanol for further experiments.

¹H NMR and ¹³C NMR:

¹H and ¹³C Nuclear Magnetic Resonance (NMR) were collected on a Bruker 500 (500 MHz) instrument. The spectra were referenced to the residual solvent signal (CDCl₃) at δ 7.26 ppm and δ 77.16 ppm respectively.

Mass Spectrometry:

High resolution mass spectroscopy was acquired with a Waters Model QTOF Ultima instrument in a positive mode at an energy of 5 V with an electrospray as the ionization source (3.5 kV) using acetonitrile as a solvent.

Work-up procedure for α-heteroarylation:

After the reaction period, the reaction mixture was transferred to a separatory funnel. The reaction vessel was rinsed with 20 mL of ethyl acetate and the organic layer was washed with 25 mL of brine (3×). The brine extractions were in turn washed with 20 mL of ethyl acetate and the combined organic phases were dried over sodium sulfate. The product was then concentrated in vacuo and 1,3,5-trimethoxybenzene (TMB) was added as an internal standard to calculate the yield through ¹H NMR. Briefly, TMB (12 mg) was added to the product and the mixture was dissolved with CDCl₃. The ¹H NMR spectrum was acquired with a 5 s relaxation delay between scans.

The product was isolated from the starting materials through column chromatography using silica (43-60 μm) with toluene as the mobile phase.

Gibbs Free Energy for Photoinduced Electron Transfer:

The Gibbs free energy for photoinduced electron transfer can be computed using the following equation:³

$$\Delta G_{ox}^o = E_{D/D^+} - E_{A/A^-} - E_{0,0} - \frac{e^2}{\epsilon r} \quad \text{(Eqn. S1)}$$

where F is the Faraday constant (23.061 kcal V⁻¹ mol⁻¹), E_{red} and E_{ox} are the redox potentials for the species undergoing the redox reaction, E_{0,0} is the excited state energy, and e²/εr accounts for the solvent-dependent energy difference due to the Coulombic effect on the charge separation.

$$\Delta G_{ox}^o = +0.42 V - (-2.44 V) - 3.00 V - \frac{(1.602 * 10^{-19} C)^2}{37.8 F m^{-1} * (462 * 10^{-12} m)}$$

$$\Delta G_{ox}^o = -0.14 kcal/mol$$

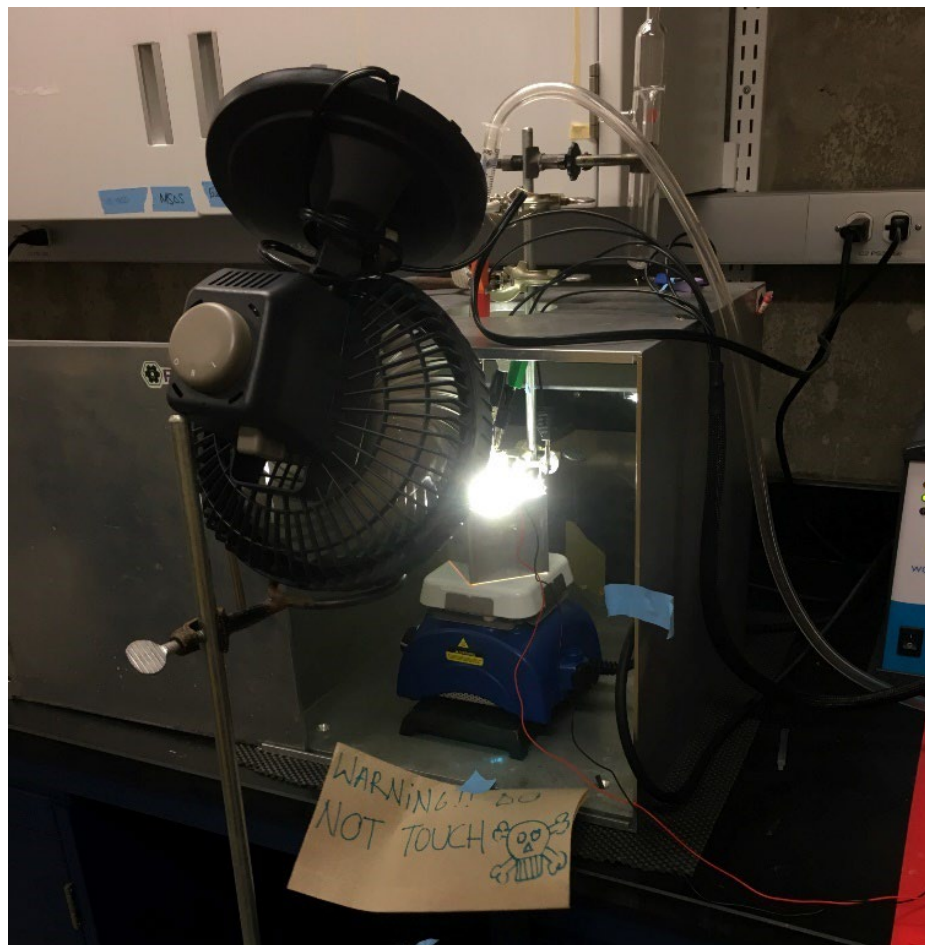


Figure S1. Picture of the reaction setup. The reaction vessel is clamped inside a home build photoreactor and above a stirring plate. A three-electrode system is set up to monitor the reaction through a bulk electrolysis experiment. Argon is bubbled into the solution throughout the whole reaction and a fan is placed in front of the setup to cool the photoreactor and to maintain the temperature of the reaction at 23 °C.

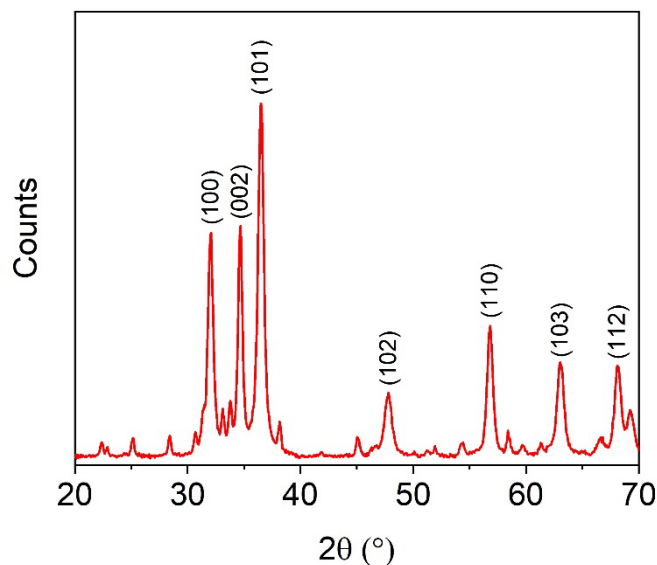


Figure S2. PXRD diffractogram for the ZnO NPs. The diffractogram shows crystalline reflections for the (100), (002), (101), (102), (110), (103), and (112) planes. This pattern agrees with the literature values for wurtzite ZnO.⁴

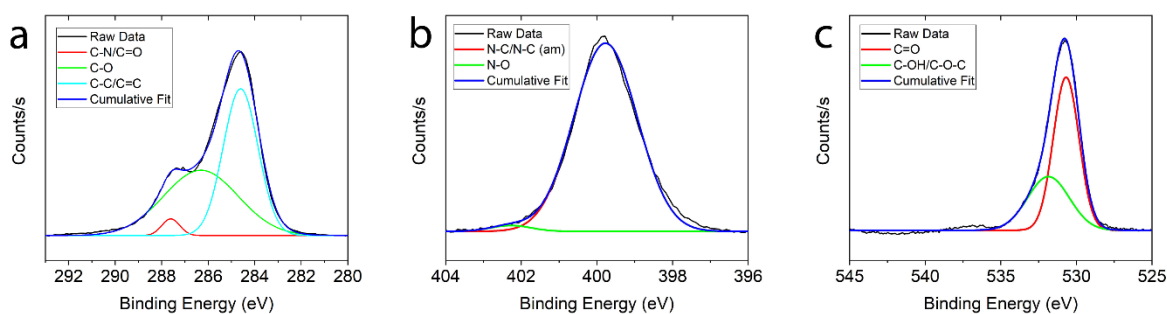


Figure S3. HR-XPS for: a) C1s; b) N1s; and c) O1s

Table S1. Wavenumber assignments for the PD2-CDs FTIR

<i>Wavenumber (cm⁻¹)</i>	<i>Assignment</i>
1213	v Acyl C-O
1364	v Amide C-N
1532	v Carboxyl C=O
1556	v Amide C=N
1632	v Amide C=O
2977	v Alkyl C-H
3500-3000	v Surface O-H

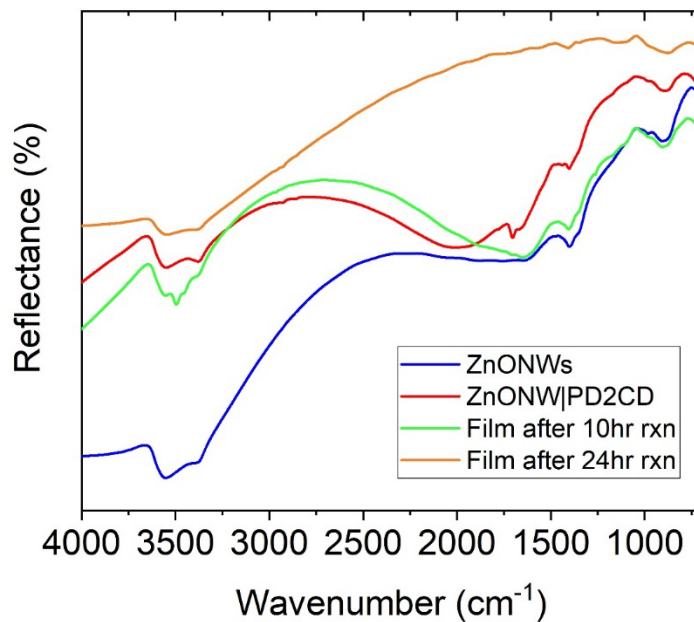


Figure S4. Diffuse reflectance infrared Fourier transform spectra for the ZnO NWs (blue trace) and functionalized films before (red trace) and after a 10 (green trace) and 24 (orange trace) hr reaction.

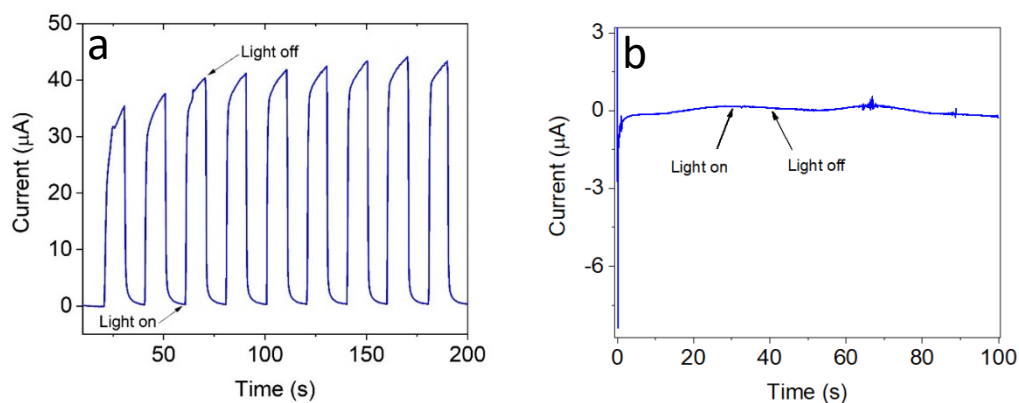


Figure S5. Chronoamperogram for the ZnO NWs upon (a) UV-light ($\lambda_{\text{ex}} = 365 \text{ nm}$) and (b) white light illumination. RE: Ag/AgCl, CE: Pt wire, WE: film of ZnO NWs in 0.1 M KCl.

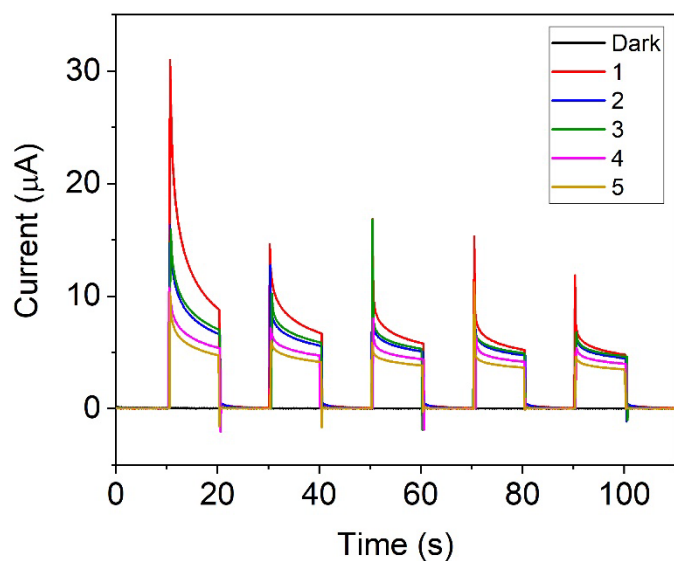


Figure S6. Chronoamperometry experiments in five fresh electrolyte solutions for five light on-off cycles each. There is no significant decrease in current which confirms a strong attachment between the **PD2-CDs** and the ZnO.

Table S2. Current density data for Figure S6.

Solution	Cycle 1 (%)	Cycle 2 (%)	Cycle 3 (%)	Cycle 4 (%)	Cycle 5 (%)
1	100	100	100	100	100
2	68.22	79.97	84.73	88.77	91.84
3	72.12	84.60	88.67	91.76	94.95
4	53.01	66.07	72.40	77.10	80.84
5	46.59	58.05	62.80	66.87	70.32

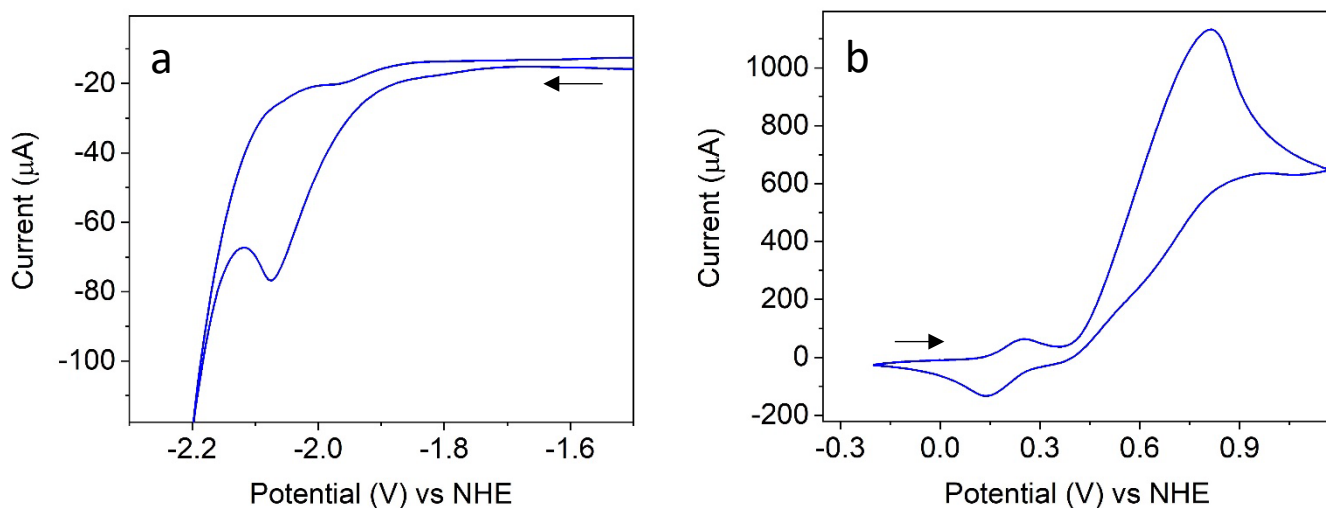


Figure S7. Electrochemical characterization of the starting materials through cyclic voltammetry; a) reduction scan of 2-chlorobenzothiazole; b) oxidation scan of 1-phenylpyrrolidine. RE: Ag wire, CE: Pt wire, WE: glassy carbon, 0.1 M TBAPF₆ in acetonitrile (scan rate: 100 mV/s).

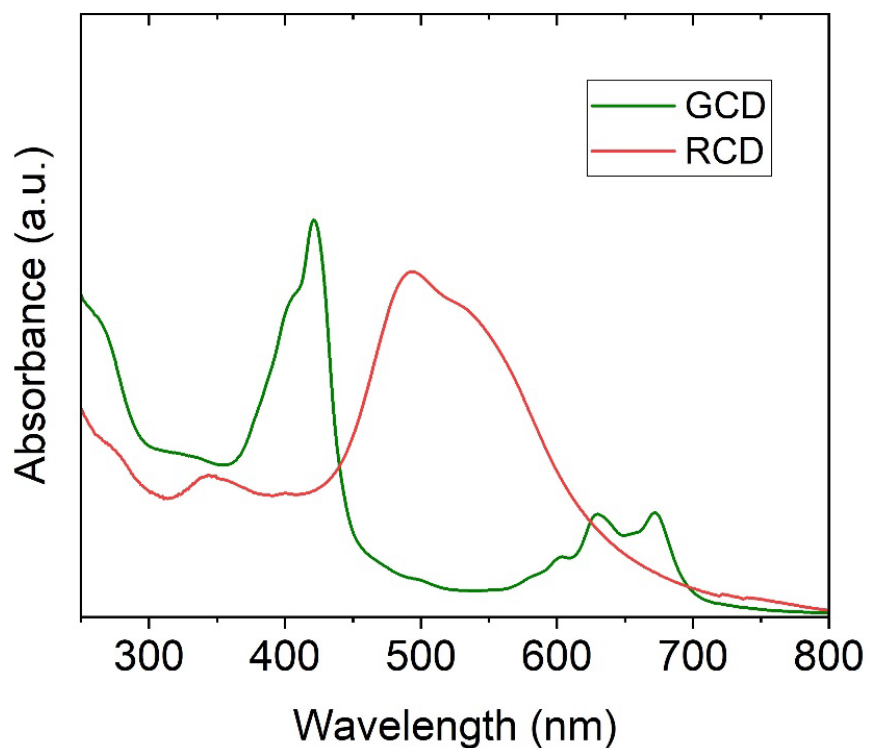


Figure S8. Absorption spectra for the GCDs (green trace) and RCDs (red trace) dispersed in water.

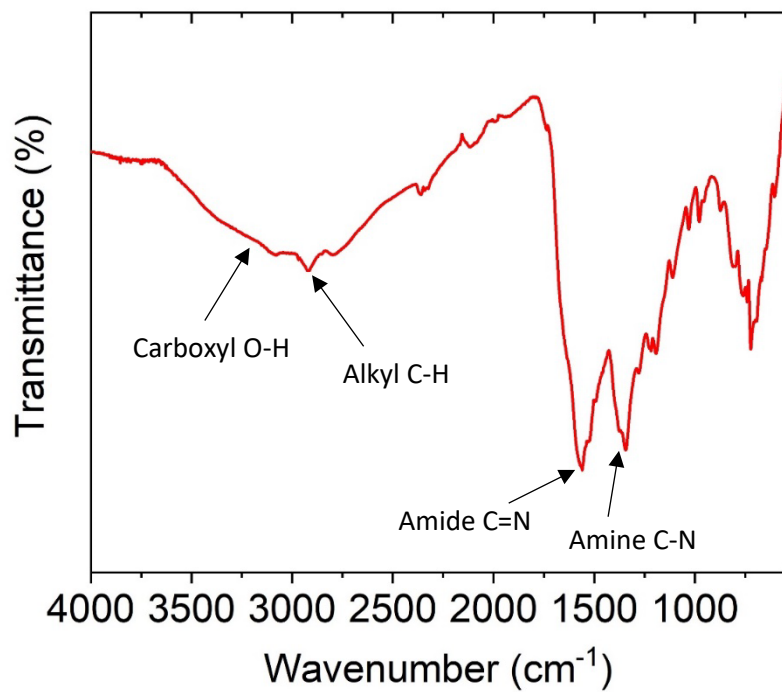


Figure S9. FTIR spectrum for the RCDs.

Table S3. Wavenumber assignments for the FTIR of RCDs

<i>Wavenumber (cm⁻¹)</i>	<i>Assignment</i>
1374	v Amine C-N
1562	v Amide C=N
2923	v Alkyl C-H
3500-3000	v Surface O-H

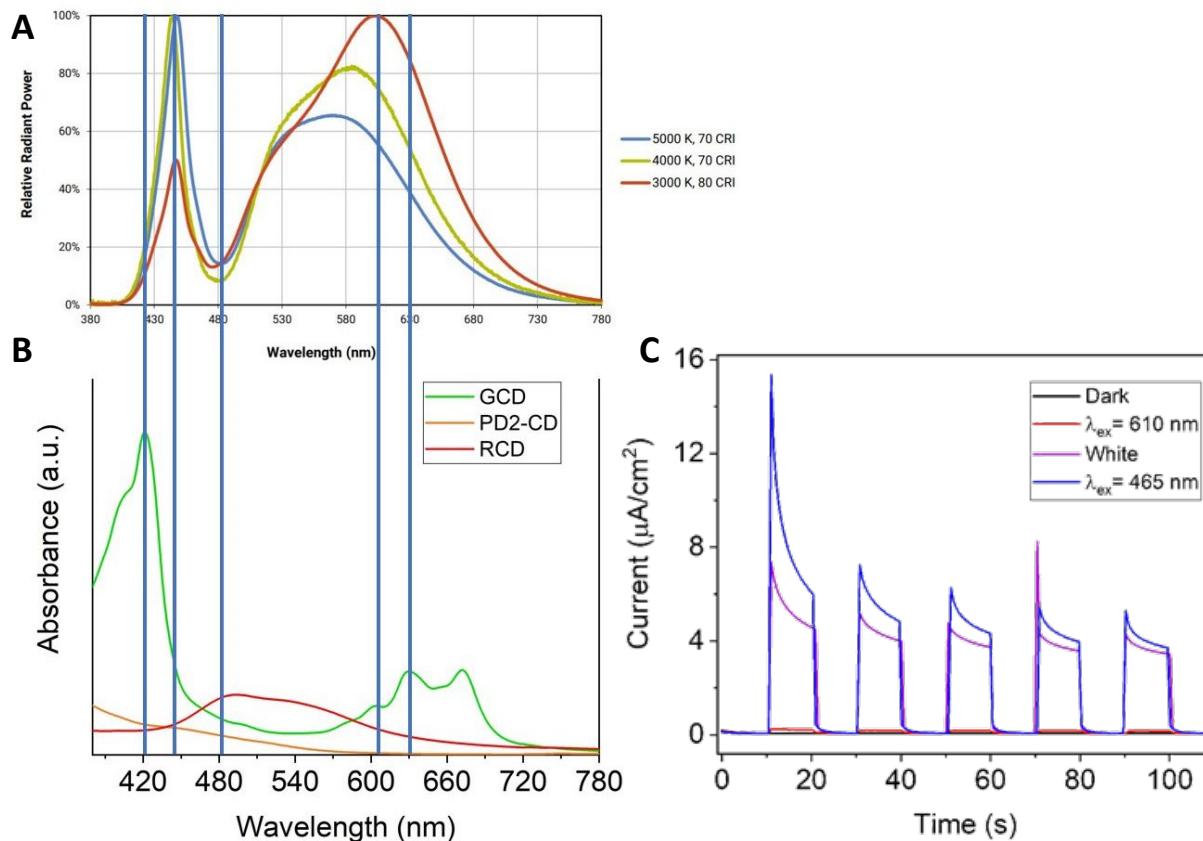


Figure S10. A) The emission profile for the white LEDs is matched to the B) absorbance spectra of the three different types of CDs used in this work. The blue component of the LEDs matches the shoulder of the PD2-CDs. C) Chopped-light chronoamperometry experiment with **ZnO NWs|PD2-CDs** films under varying LED illumination (white light LEDs, purple trace; red LEDs, red trace; blue LEDs, blue trace). Irradiation with red LEDs yields low photocurrent compared to white and blue LEDs.

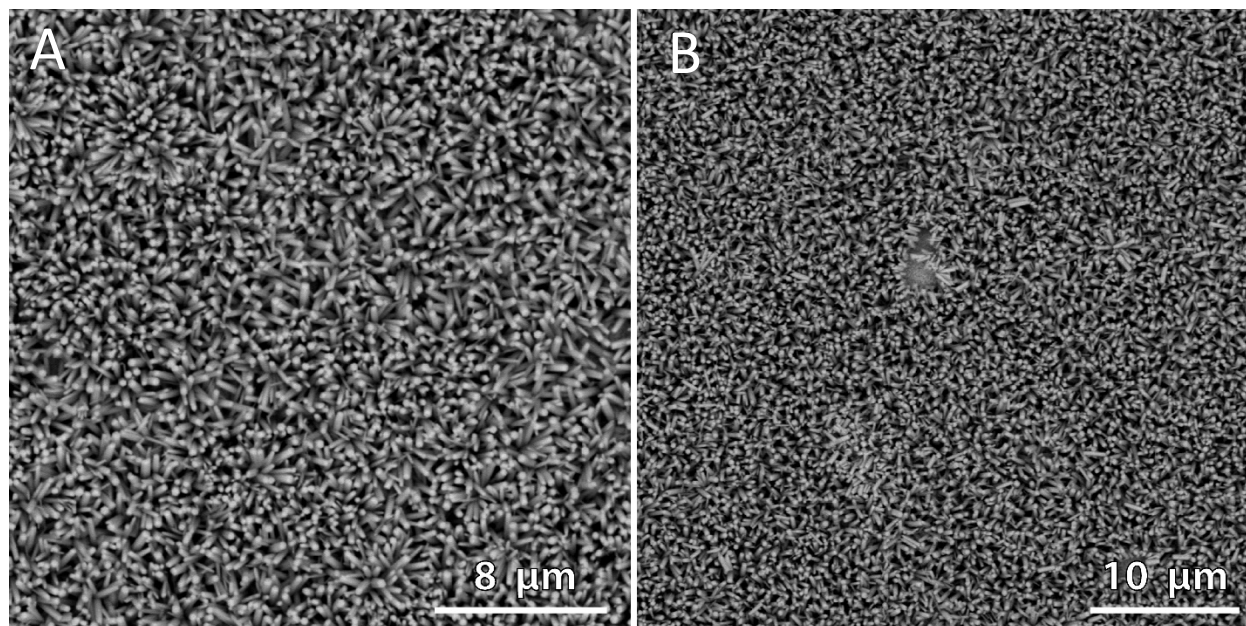


Figure S11. SEM images of the film (a) before and (b) after a 10 hrs reaction. The NWs remain in good condition.

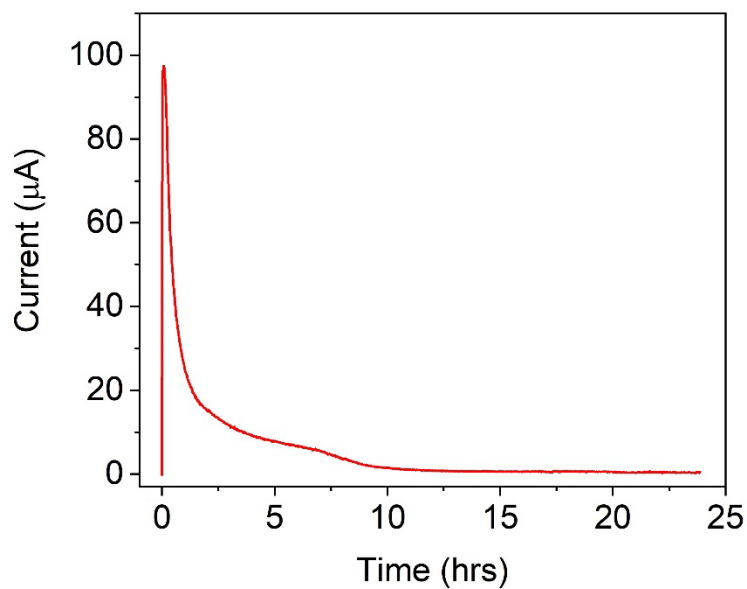


Figure S12. Bulk electrolysis experiment without applied bias. This experiment was performed to monitor the course of the reaction. There is a large increase in current in the first 30 min of the reaction due to a high charge buildup caused by the oxidation of the 1-phenylpyrrolidine at the film/solution interface. The current throughout the film stabilizes after ca. 2.5 hrs and at 10 hrs there is no significant oxidation observed and the reaction is nearing completion.

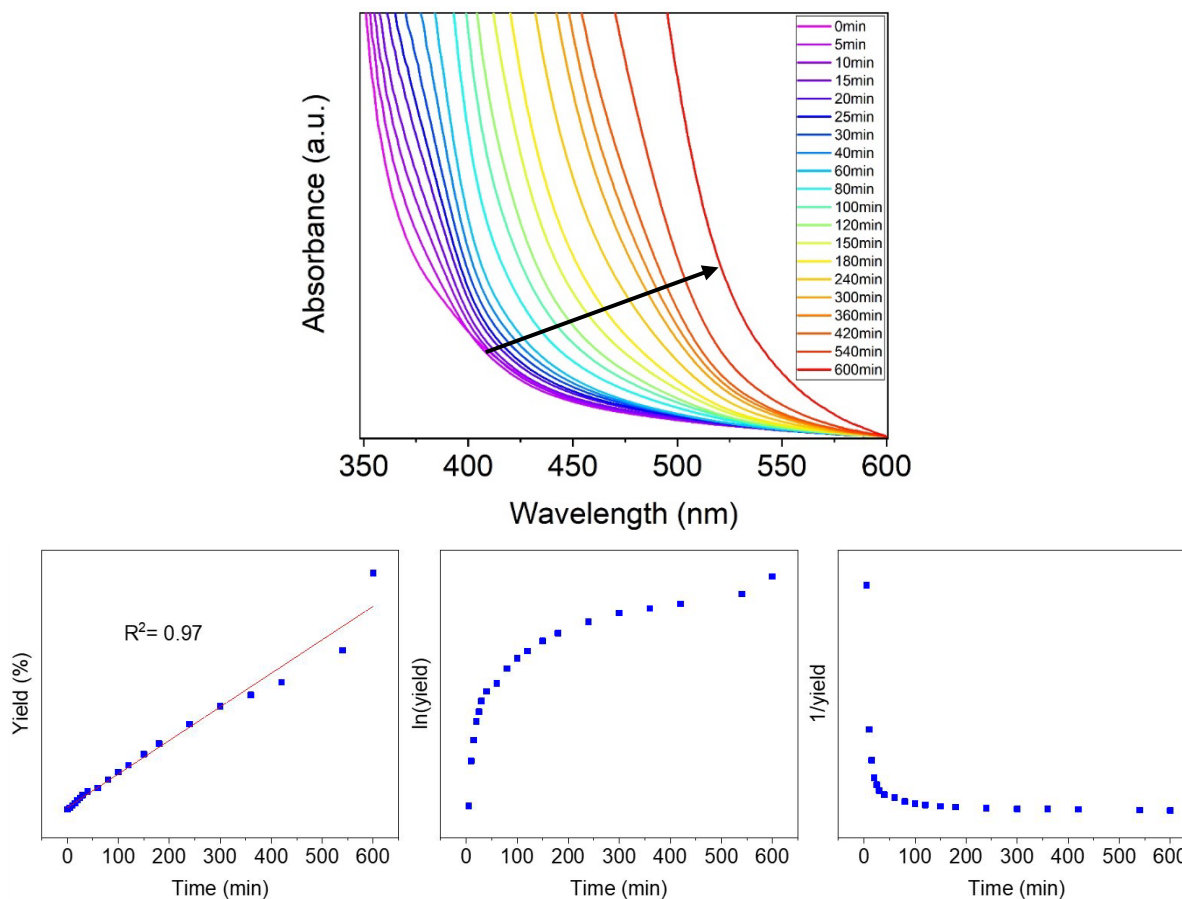


Figure S13. Time-course UV-Vis experiment for the evaluation of the kinetics of the reaction. The reaction proceeds in a steady fashion throughout 10 hr of reaction following zero-order kinetics.

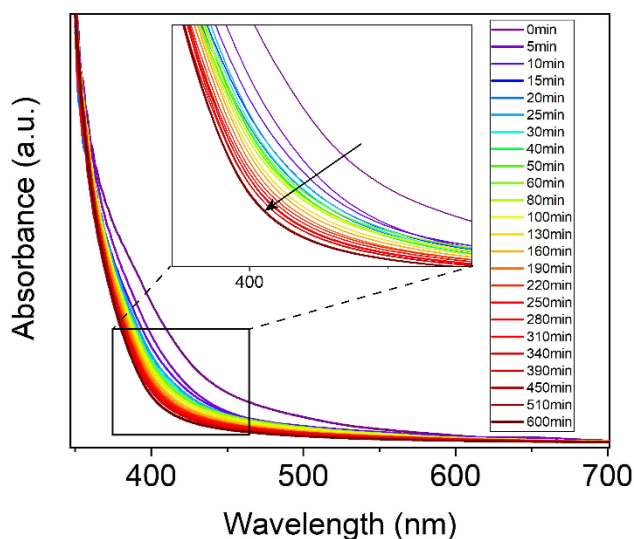


Figure S14. Time-course UV-Vis experiment for the oxidation of 1-phenylpyrrolidine without the presence of 2-chlorobenzothiazole. There is a rapid decrease in the concentration of the amine in the first 15 min correlating to the bulk electrolysis experiment (Figure S12). There is a steady decrease in the absorbance following this rapid decrease in the concentration.

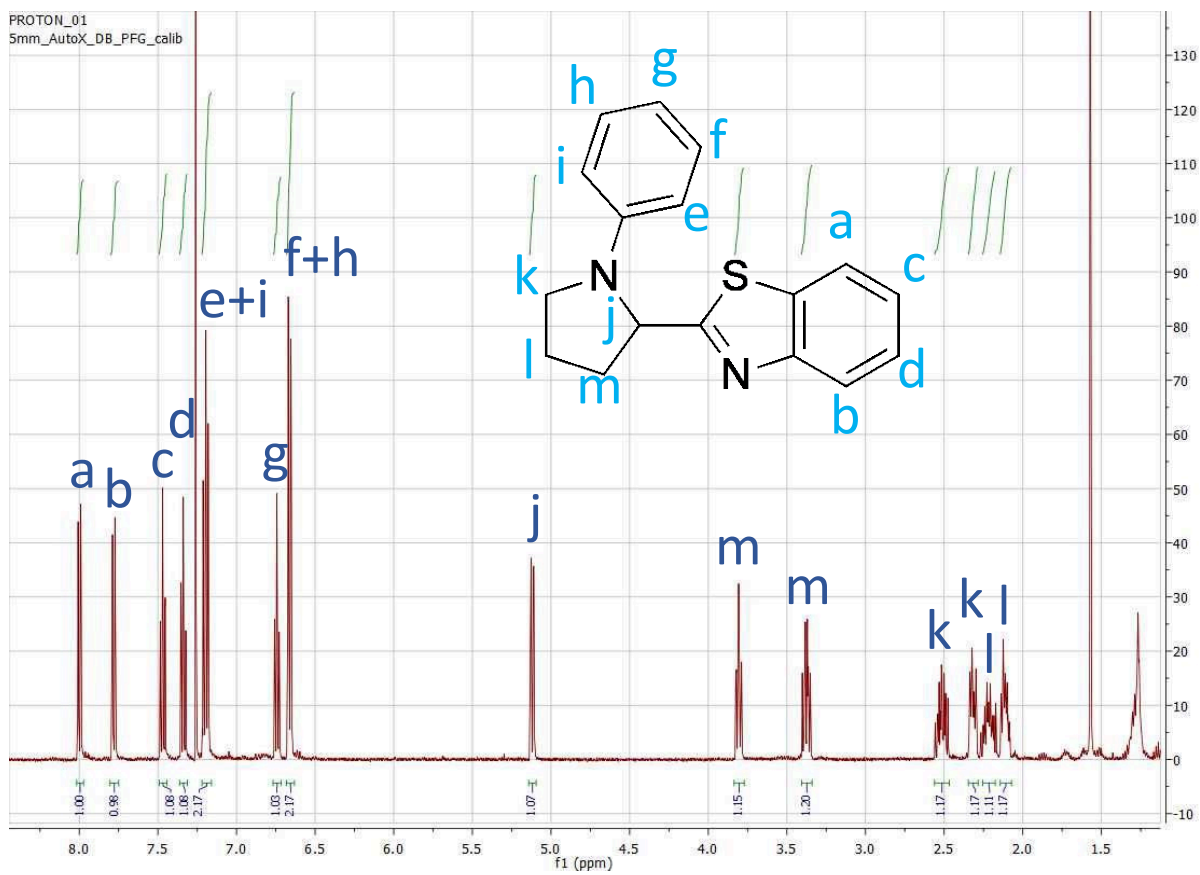


Figure S15. ^1H NMR **3** (500 MHz, CDCl_3): δ 8.00 (d, 1H_a), 7.78 (d, 1H_b), 7.48 (dd, 1H_c), 7.34 (dd, 1H_d), 7.20 (dd, 2H_e), 6.75 (t 1H_f), 6.66 (d, 2H_g), 5.12 (d, 1H_h), 3.81 (dd, 1H_i), 3.37 (m, 1H_j), 2.56 – 2.46 (m, 1H_k), 2.32 (m, 1H_l), 2.27 – 2.16 (m, 1H_m), and 2.11 (m, 1H_n).

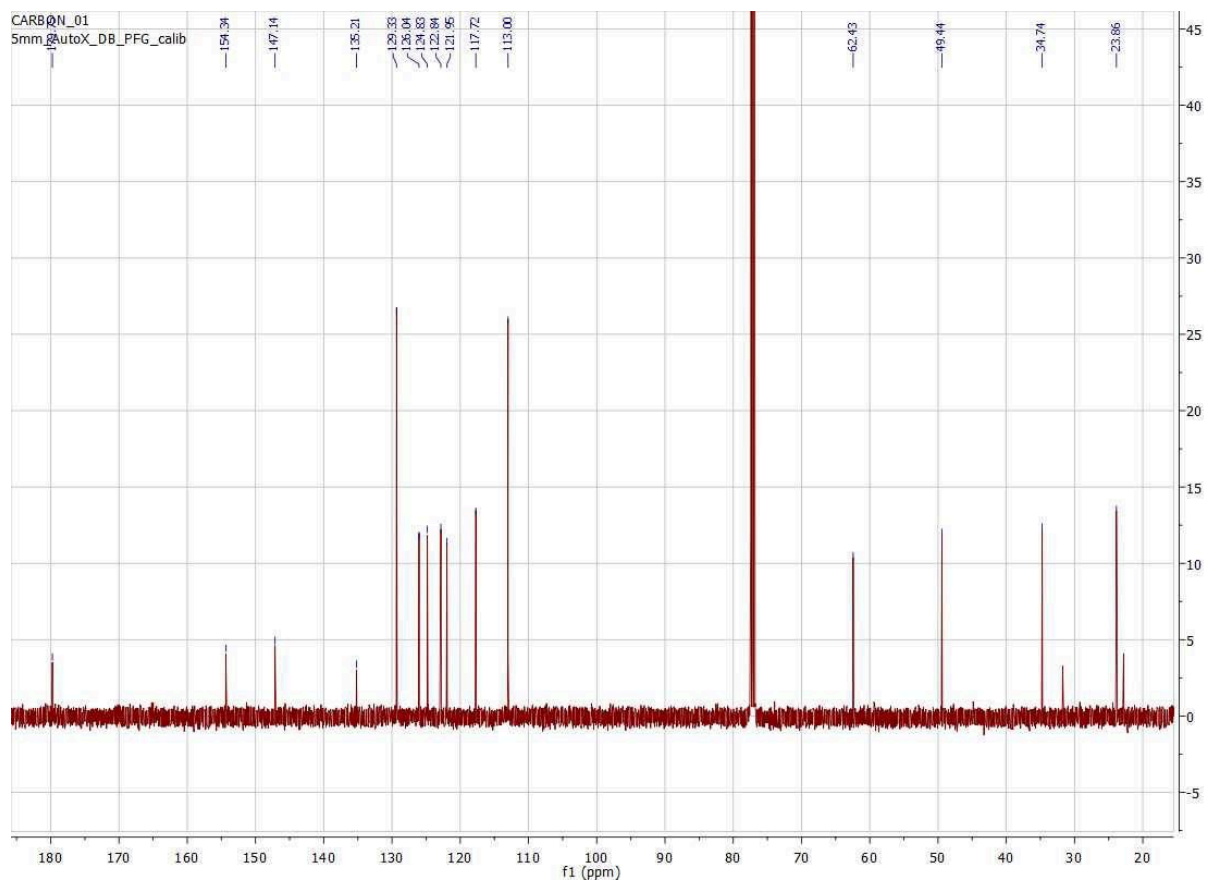


Figure S16. ^{13}C NMR **3** (500 MHz, CDCl_3): δ 179.8, 154.3, 147.1, 135.2, 129.3, 126.0, 124.8, 122.8, 122.0, 117.7, 113.0, 62.4, 49.4, 34.7, 23.9.

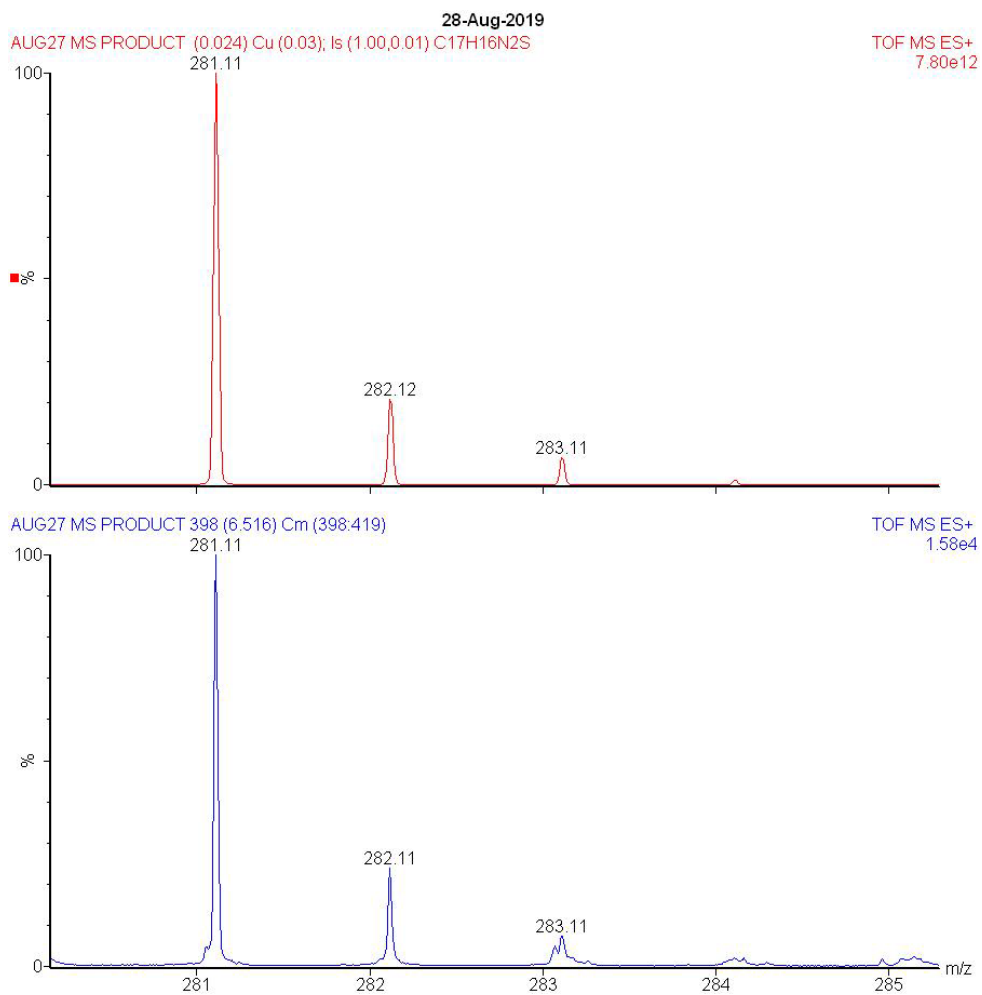


Figure S17. Mass spectrum for the isolated product **3** in acetonitrile. We observe that the predicted pattern in red (top) matches the pattern from **3** in blue (bottom) at $[M+H]^+=281.11$ m/z .

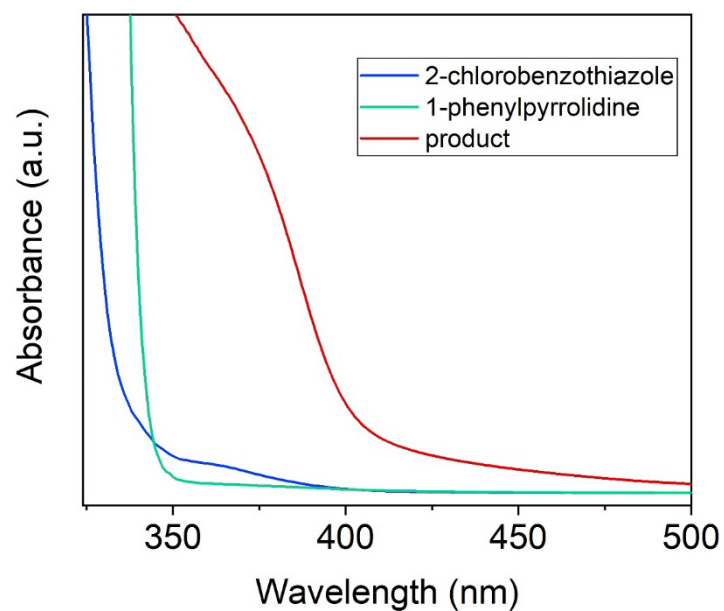


Figure S18. UV-vis spectrum for the starting materials 1-phenylpyrrolidine (**1**) and 2-chlorobenzothiazole (**2**), and 2-(1-phenylpyrrolidin-2-yl)benzo[d]thiazole (**3**). The spectrum for **2** shows an absorption maximum at 360 nm with a shoulder that extends to 400 nm.

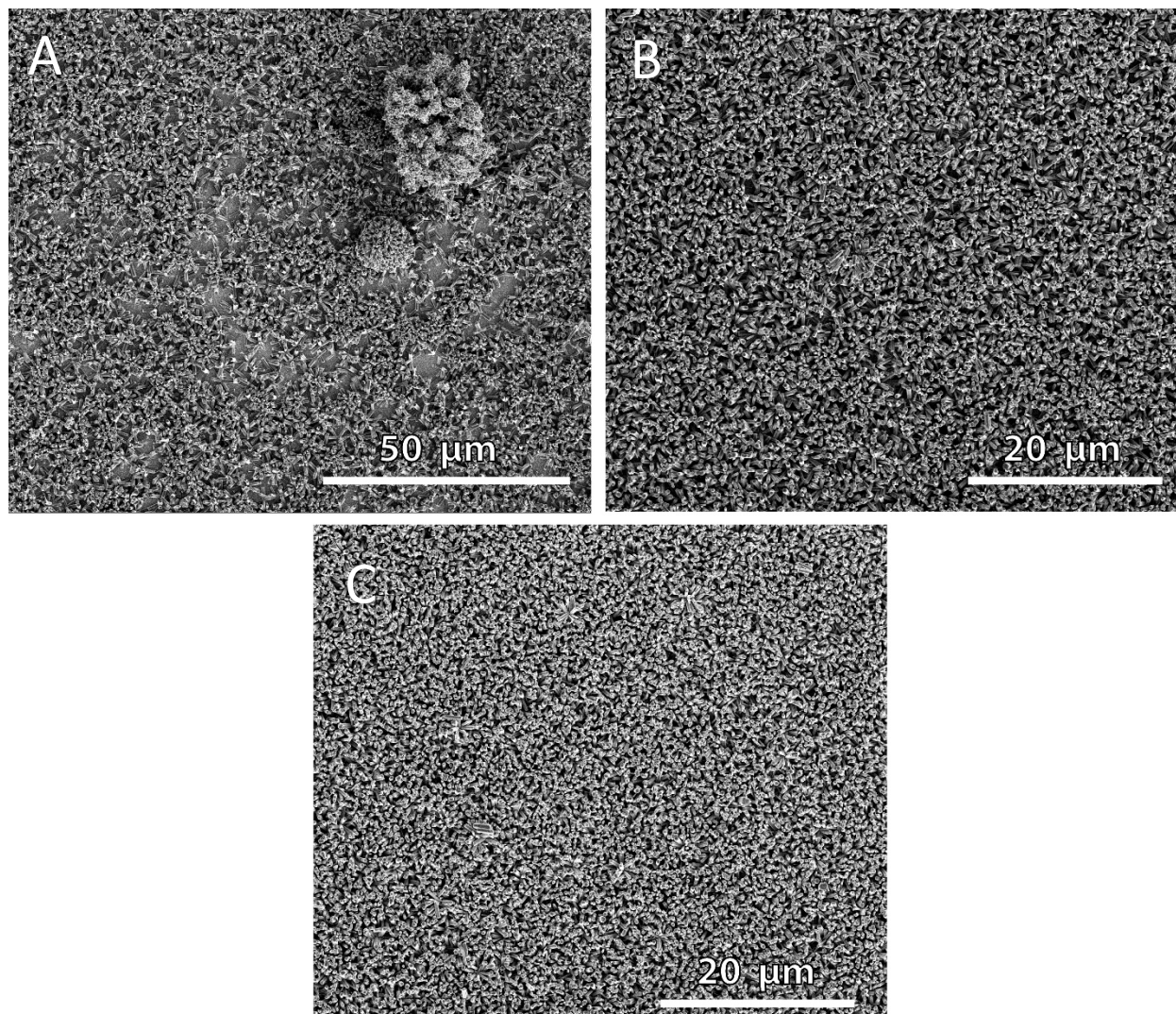


Figure S19. SEM images for ZnO NW films grown from a) 2; b) 4; c) 6; drops of seeding solution. As the number of drops increase, the roughness decreases and wire density/uniformity increase.

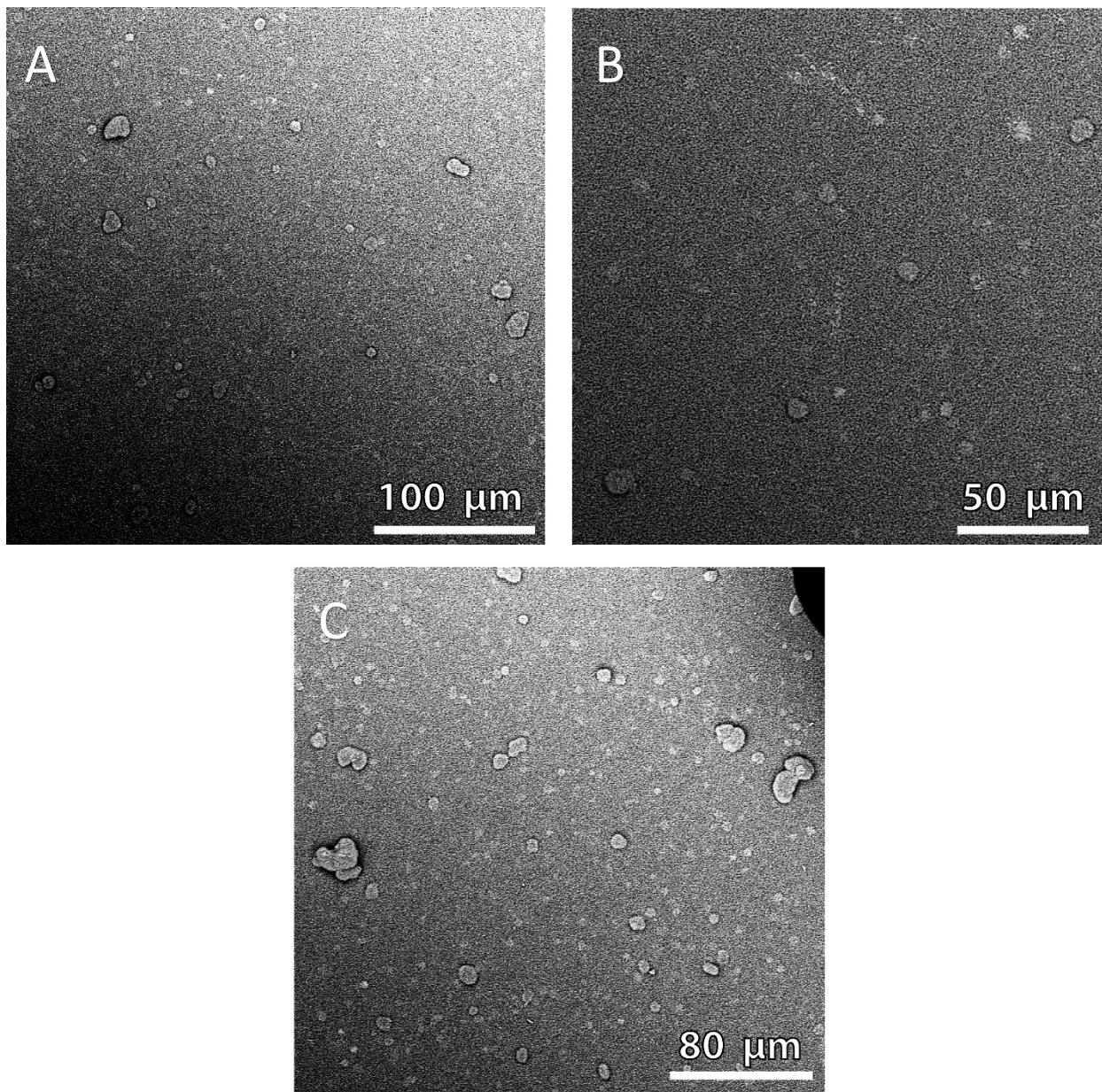


Figure S20. SEM images for ZnO NW films grown from a) 10; b) 20; c) 40 drops of seeding solution. Here the roughness and aggregation increase as the number of seeding solution drops increases.

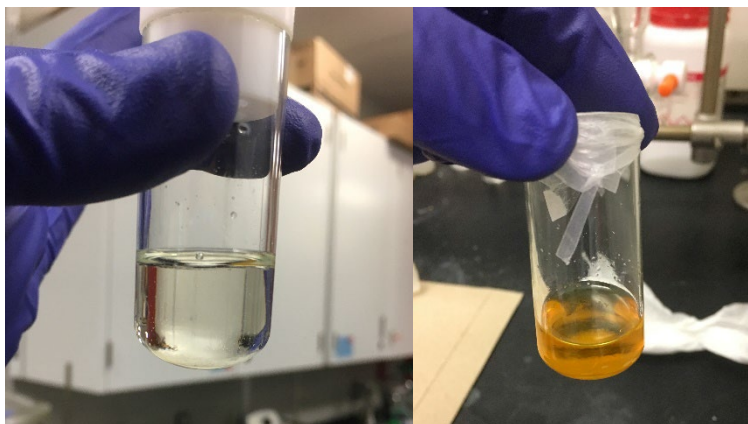


Figure S21. Picture of the solution before and after the reaction of **1** and **2** to form **3**.

References

1. Hu, Y.; Jiang, Z.; Xu, C.; Mei, T.; Guo, J.; White, T., Monodisperse ZnO Nanodots: Synthesis, Characterization, and Optoelectronic Properties. *The Journal of Physical Chemistry C* **2007**, *111* (27), 9757-9760.
2. Yarur, F.; Macairan, J.-R.; Naccache, R., Ratiometric Detection of Heavy Metal Ions Using Fluorescent Carbon Dots. *Environmental Science: Nano* **2019**, *6* (4), 1121-1130.
3. Romero, N. A.; Nicewicz, D. A., Organic Photoredox Catalysis. *Chemical Reviews* **2016**, *116* (17), 10075-10166.
4. Omri, K.; Alyamani, A.; El Mir, L., Surface Morphology, Microstructure and Electrical Properties of Ca-Doped ZnO Thin Films. *Journal of Materials Science: Materials in Electronics* **2019**.